Soliton dynamics in a microstructured lattice model

1991 J. Phys. A: Math. Gen. 24 2151

(http://iopscience.iop.org/0305-4470/24/9/023)

J. Phys. A: Math. Gen. 24 (1991) 2151–2172. Printed in the UK

Soliton dynamics in a microstructured lattice model

M K Sayadi and J Pouget

Laboratoire de Modélisation en Mécanique (associé au CNRS), Université Pierre et Marie Curie, Tour 66, 4 Place Jussieu, 75252 Paris Cédex 05, France

Received 26 November 1990

Abstract. The nonlinear dynamics of localized structures of the soliton type in a lattice model involving internal degrees of freedom in rotation is presented. The physical model consists basically of a one-dimensional monoatomic chain equipped with microscopic electric dipoles associated with molecular groups. The model is particularly suitable for molecular ferroelectric crystals such as sodium nitrite exhibiting structures in ferroelectric domains and walls or for long chains of polymers such as crystalline polyethylene or polyvinylidene fluoride and others where molecular groups perform rotational motions. Two main types of motion can be distinguished in this picture: (i) the longitudinal and transverse displacements of the mass centre of the molecular group and (ii) two rigid-body rotational motions of the electric dipoles about the chain axis and perpendicular to it.

The propagation of coupled solitons is investigated for two elementary configurations. A situation for which all the dipoles rotate perpendicularly to the chain axis is first studied. A second configuration is next considered when the dipole rotation takes place about the chain axis. For both configurations and from the continuum approximation framework the existence of coupled solitons in rotation and lattice deformation are proved and the role played by the coupling between rotation and displacements are placed in evidence leading to particularly interesting soliton solutions. The set of nonlinear equations is made of (i) the wave equations for the elastic displacements and (ii) an equation of the sine-Gordon type being nonlinearly coupled. The soliton solutions, thus obtained, can be interpreted as the motion, coupled to the elastic behaviour, of a domain wall in a ferroelectric crystal or as the motion of a twist defect in a long deformable chain of macromolecules for polymer materials. For each situation and soliton solution, the energy of the system as well as the soliton width are given. The most meaningful results are illustrated by means of numerical simulations.

1. Introduction

The main purpose of this paper is to construct and investigate a lattice model exhibiting particularly interesting *nonlinear phenomena* connected with *internal degrees of freedom* inherent to a refine description of the material. The basic lattice model consists of a chain of particles which cannot be reduced to a point endowed with a simple mass, but the particle displays an *angular momentum.* The latter is, of course, due to the additional degrees of freedom which are placed in evidence by considering fine kinematic description involving rotational motions. A good picture of such media can be provided by a deformable lattice equipped, at each of its nodes, with molecules performing rigid-body rotational motions about their mass centre [1, 2]. Therefore, in addition to the usual particle displacements we must take the *microgyration of the molecules* into account. However, the nonlinear dynamics of such a lattice requires interactions which depend on the physics of the microsystem being considered. Then, such microstructured lattices are models for molecular ferroelectric crystals of which

0305-4470/91/092151+22$03.50

sodium nitrite is a good prototype [3-5]. The model is also suitable for the study of twist defects in a long chain of polymer where the molecular structure involves rotational degrees of freedom, and thus crystalline polyethelene [6], polyvinyline fluoride [7] or polytetrafluoroethylene [8] are good examples of polymers. Moreover, the model can be extended to long chains of biological macromolecules called DNA which have a helical structure including internally rotational motions [9-11]. On the basis of the microstructured lattice model, we aim at examining the propagation of nonlinear excitations of the soliton type. To be more precise we attempt to prove the existence of kink defect motions as *coupled solitons in rotation-deformation.*

Ordered-disordered structures relating to phase transitions in crystals often involve microstructured lattices such as chains of magnetic spins in ferromagnetic crystals [12, 13] or microscopic electric dipoles in ferroelectric crystals [14, 15]. Furthermore, different ordered arrangements are separated by *localized structures or domain walls* which are able to move by applying an appropriate field for instance. Domain walls appear as defects breaking the well-ordered arrangement of dipoles. Then, the dynamics of such 'wall defects' can be studied as coherent structures of the soliton type which propagate keeping their own characteristic properties (velocity, shape, etc.). In the present work, special attention is devoted to molecular crystals for which a microscopic electric dipole is rigidly attached to the molecular group—the microstructure—and the latter plays the role of 'spin'. Except for differing physical interpretations, the motion of domain walls in ferroelectric crystals can be compared to the motion of Bloch or Néel walls in ferromagnets for which the orientation of magnetic spins, within the wall thickness, evolves by rotations parallel (Bloch wall) or perpendicular (Néel wall) to the plane of the wall [16, 17].

We concentrate, here, on a lattice model for which the molecular interactions involving internal degrees of freedom in rotation are described by the dipole-dipole interactions including anisotropic effects. These interactions are obviously added to the usual interatomic forces acting between lattice particles, so that couplings between the lattice displacements and rotational motions of the molecular groups are accounted for. The equations governing the physical system are nonlinear and dispersive. Accordingly, we may obtain soliton solutions which describe the coupled motions in molecule rotations and lattice deformations. Nevertheless, because the nonlinear difference-differential equations ruling the microscopic model are not tractable, we must consider the *continuum approximation.* Then, the set of nonlinear equations thus obtained seems to be of particular interest, because of the coupling between the *wave equations* for the elastic displacements and *sine-Gordon equations* for the molecule rotations, these equations being coupled through the rotation-displacement couplings. Furthermore, these nonlinear coupled equations permit the propagation of nonlinear excitations of the soliton type. The soliton concept occupies a key position in various fields of physics [18, 19] (nonlinear optics, plasma physics, hydrodynamics, biological materials, condensed matter physics, etc.) and the present study illustrates some ideas of nonlinear science which allow one to model the nonlinear dynamics of the real world.

The nonlinear problems that we want to tackle will be carried out by considering a lattice model which consists of a simple deformable atomic chain equipped with microscopic electric dipoles. Each dipole is, in fact, associated with a molecular group which performs large rotational motions. Therefore, an angular momentum is defined. Particular attention is paid to molecular interactions, which are provided by *dipole-dipole interactions* extended to *anisotropic effects* due to the neighbouring atomic chains. The lattice model can be also compared, in its continuum approximation, to a more

general theory of *continua with microstructure* [20, 21]. More precisely, such a microstructure involving internal degrees of freedom is kinematically described, in some abstract manner, by means of a vector field, called a director, which is attached to each material point in the deformable continuum [21, 22]. The material points of the medium are endowed with a tensor of inertia in addition to the usual mass density. In the framework of the present lattice model, the notion of a director field is identified with the dipoles and a continuous density of molecular rotations can be defined. However, the comparison is well established in the context of the nonlinear theory of oriented media for which the existence of solitons in rotation and deformation has been proved [23, 24].

We begin, in section 2, with the description of a simple one-dimensional lattice model equipped with rotatory electric dipoles. Despite the overall simplicity this leads to a model which is rich enough to allow a detailed analysis of interesting nonlinear phenomena. On introducing appropriate interatomic and intermolecular interactions, we build up the Hamiltonian of the discrete system. Two simple configurations are deduced from the model next. A first situation referred to as A, for which the dipole rotation takes place about an axis perpendicular to the chain axis, is presented in section 3. The equations of motion specialized for this configuration are given in a subsection. The continuum approximation of the microscopic model yields a set of nonlinear coupled equations which consists of two wave equations for the longitudinal and transverse elastic waves nonlinearly coupled to a sine-Gordon equation for the rotational motion of the dipoles. The problem of stationary wave solutions allows one to place different kinds of coherent structures in evidence. A second configuration corresponding to the rotation of the dipoles about the chain axis is investigated in section 4. The way of solving this situation is similar to that of the first one and we also obtain coupled solitons in rotation and deformation. Finally, some concluding remarks are drawn in section 5; some extensions of the model and other problems relating to nonlinear phenomena in microstructured lattices are evoked as well.

2. Description of the model

Let us consider a one-dimensional monoatomic chain made of N particles (N can be large enough in order to avoid any boundary effects) and equipped, at each node, with a molecular group (see figure 1(a)). We propose next that each molecular group is endowed with a microscopic electric dipole of constant length which indicates the molecule orientation. The model thus built is suitable for ferroelectric molecular crystals such as sodium nitrite ($NaNO_2$) for which the nitrite group (NO_2^-) can be considered as a small rigid-body surrounded by four sodium (Na^+) ions. Moreover, the motions of the NO_2^- group relative to the Na^+ ions can be neglected in the first approximation, since these relative motions would yield very high frequencies [3–5, 25]. The lattice model can also correspond to chains of polymers such as crystalline polythylene where the CH_2 molecule suffers a rotation about the chain axis [6, 26]. Polyvinylidene fluoride (PFV$_2$) [7] or polytetrafluoroethylene (PTFE) where the CF_2 units are subject to rotational motions [8, 27] are also good candidates for our model. Furthermore, extension of the model to biological materials such as DNA can be considered [10, 11].

Accordingly, we can reduce the crystal cell to a point equipped with the global mass of the cell at its mass centre. Moreover, in order to account for the molecular

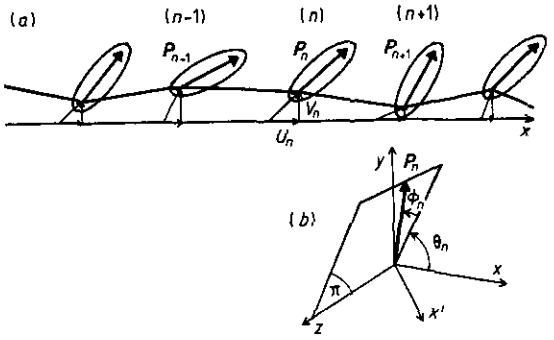

Figure 1. Lattice model: (*a*) one-dimensional atomic chain equipped with rotatory molecular groups (microstructures), (*b*) angles of rotations for the dipoles or molecular groups. θ_n, rotation about the z axis; φ_n, rotation about the x' axis.

group, rotatory microscopic electric dipoles are added to each lattice point. The forces acting on the system result from (i) the ionic interactions between neighbouring particles as in classical ionic crystals, (ii) the mutual interactions between microscopic dipoles and (iii) the electrostatic interactions due to the external field $\boldsymbol{E}$. On the other hand, the possible motions of the lattice are (i) the *longitudinal* and *transverse displacements* of the mass centre of the nth crystalline cell denoted by U_n and V_n, respectively, and (ii) the *rigid-body rotational motions* of the microscopic dipoles or molecules. The latter can have two angles of rotation (see inset of figure 1(*b*)), the angle θ_n of the plane (Π) about the z axis and the angle φ_n corresponding to a rotation in the plane (Π) about an axis perpendicular to it. We also assume that the lattice displacements are infinitesimal whereas the rotations may have large amplitudes.

The Hamiltonian of the discrete system is classically obtained by expanding the mutual electrostatic energy between dipoles up to the first order in the lattice deformation. This allows us to place the interacting energy between the dipoles and lattice deformations in evidence [15, 28]. The Hamiltonian can be then written as the following sum:

$$H = K + W_{\text{lat}} + W_{\text{dip}} + W_{\text{int}} + W_{\text{ext}}. \tag{1}$$

The *kinetic energy* of the lattice including both translational and rotational motions is given by

$$K = \tfrac{1}{2}\sum_n (\dot{U}_n^2 + \dot{V}_n^2 + \dot{\theta}_n^2 + \dot{\varphi}_n^2) \tag{2}$$

where appropriate non-dimensional notations have been used, and the particle mass and moments of inertia have been set to unity for ease of presentation. The energy of *the deformable lattice* reads as

$$W_{\text{lat}} = \sum_n \tfrac{1}{2}[K_{\text{L}}(U_{n+1} - U_n)^2 + K_{\text{T}}(V_{n+1} - V_n)^2] \tag{3}$$

where K_{L} and K_{T} are the longitudinal and transverse coefficients of the interacting forces. The energy of the *dipole interactions* is written as

$$W_{\text{dip}} = \sum_n [\varepsilon(\boldsymbol{p}_n \cdot \boldsymbol{p}_{n+1} - 3p_n^x p_{n+1}^x) + \eta p_n^x p_{n+1}^x + \nu p_n^y p_{n+1}^y]. \tag{4}$$

We denote by $\boldsymbol{p}_n$ the unit vector such that the microscopic dipole is $\boldsymbol{P}_n = P_0 \boldsymbol{p}_n$, and p_n^x and p_n^y hold for the projections of $\boldsymbol{p}_n$ onto the x and y axis, respectively. The coefficient

$\varepsilon = P_0^2/4\pi a^3 \varepsilon_0$ corresponds to the dipole–dipole interaction in vacuum (ε_0 is the vacuum dielectric constant). *Anisotropic terms* in the x and y directions have been added in order to take the environment of the atomic chain into account. These anisotropic terms are characterized by the parameters η and ν, which allows one to favour one direction at the cost of the other one ($\eta \gg \nu$ or $\eta \ll \nu$). The *energy of interaction* between the lattice of dipoles and lattice deformation is provided by

$$W_{\text{int}} = -3\frac{\varepsilon}{a}\sum_n [(\boldsymbol{p}_n \boldsymbol{p}_{n+1} - 3p_n^x p_{n+1}^x)(U_{n+1} - U_n) + (p_n^x p_{n+1}^y + p_n^y p_{n+1}^x)(V_{n+1} - V_n)] \tag{5}$$

which is deduced from the electrostatic dipole energy. Finally, the energy due to the *external field* applied to the lattice is simply given by

$$W_{\text{ext}} = P_0 \sum_n \boldsymbol{E} \cdot \boldsymbol{p}_n \tag{6}$$

where $\boldsymbol{E}$ is the applied field.

The Hamiltonian of the system can be rewritten in terms of angles of rotations by setting

$$\boldsymbol{p}_n = (\cos\varphi_n \cos\theta_n, \cos\varphi_n \sin\theta_n, \sin\varphi_n)^{\mathrm{T}}. \tag{7}$$

At this stage of the work two elementary configurations can be extracted from the complete problem: (i) the configuration (below referred to as A) defined by putting $\varphi_n = 0$ and $\theta_n \neq 0$ (all the dipoles rotate about the z axis); and (ii) the configuration B for which the dipoles rotate about the chain axis and $\theta_n = \pi/2$. The more complex problem, where the rotations φ_n and θ_n are both considered, will be undertaken in another part of the work.

3. Coherent structures for configuration A

3.1. Equations of motion for the discrete system

On equating φ_n to zero in the energies (2)–(5), the Hamiltonian takes on the following form:

$$\begin{aligned} H_{\text{A}} = {} & \sum_n \tfrac{1}{2}(\dot{U}_n^2 + \dot{V}_n^2 + \dot{\Theta}_n^2) + \sum_n \tfrac{1}{2}[C_{\text{L}}^2(U_{n+1} - U_n)^2 + C_{\text{T}}^2(V_{n+1} - V_n)^2] \\ & + \sum_n \tfrac{1}{2}[\alpha(U_{n+1} - U_n)\cos\Theta_n - \beta(V_{n+1} - V_n)\sin\Theta_n] \\ & - \sum_n \left[4\cos\left(\frac{\Theta_{n+1} - \Theta_n}{2}\right) - \chi\cos\left(\frac{\Theta_{n+1} + \Theta_n}{2}\right)\right] \end{aligned} \tag{8}$$

where we have set

$$(K_{\text{L}}, K_{\text{T}}) = \tfrac{1}{2}(C_{\text{L}}^2, C_{\text{T}}^2)(\varepsilon - \eta - \nu) \qquad \chi = 4\frac{\eta - \nu - 3\varepsilon}{\varepsilon - \eta - \nu}$$

$$\alpha = \frac{18\varepsilon}{a(\varepsilon - \eta - \nu)} \qquad \beta = \tfrac{2}{3}\alpha$$

and the new scale time $t\sqrt{(\varepsilon-\eta-\nu)/2}$ has been introduced where $\varepsilon-\eta-\nu>0$ has been assumed. Moreover, the external field has been dropped and we have set $\Theta_n=2\theta_n$. The Euler-Lagrange equations can be derived from (8) and they read as

$$\ddot{U}_n - C_L^2(U_{n+1}+U_n-2U_n)=\tfrac{1}{2}\alpha(\cos\Theta_{n+1}-\cos\Theta_{n-1}) \tag{9a}$$

$$\ddot{V}_n - C_T^2(V_{n+1}+V_n-2V_n)=-\tfrac{1}{2}\beta(\sin\Theta_{n+1}-\sin\Theta_{n-1}) \tag{9b}$$

$$\ddot{\Theta}_n - 2[\sin\tfrac{1}{2}(\Theta_{n+1}-\Theta_n)-\sin\tfrac{1}{2}(\Theta_n-\Theta_{n-1})]$$

$$=\frac{\chi}{2}[\sin\tfrac{1}{2}(\Theta_{n+1}+\Theta_n)+\sin\tfrac{1}{2}(\Theta_n+\Theta_{n-1})]$$

$$+\tfrac{1}{2}\alpha(U_{n+1}-U_{n-1})\sin\Theta_n+\tfrac{1}{2}\beta(V_{n+1}-V_{n-1})\cos\Theta_n. \tag{9c}$$

The study of the set of difference-differential equations is not tractable in an analytical way, the nonlinear dynamics of such discrete equations can be, however, solved by means of numerical investigations by using well-defined initial and boundary conditions. Nevertheless, we adopt the continuum approximation in order to get some more precise information about the solutions.

3.2. Continuum approximation

We suppose now that the discrete displacements and rotations are slowly varying over a crystalline spacing. Furthermore, the attention is focused on dynamic processes of spatially extended waves. After some classical manipulations where we have supposed that $|\chi|\ll 4$ and expanded the discrete functions in Taylor series around $x=na$, we obtain

$$U_{tt}-C_L^2U_{xx}=\alpha(\cos\Theta)_x \tag{10a}$$

$$V_{tt}-C_T^2V_{xx}=-\beta(\sin\Theta)_x \tag{10b}$$

$$\Theta_{tt}-\Theta_{xx}=\chi\sin\Theta+\alpha U_x\sin\Theta+\beta V_x\cos\Theta. \tag{10c}$$

The change of space variable $X=x/a$ has been introduced. These equations can be deduced from the following Hamiltonian density:

$$h_A-h_0=\tfrac{1}{2}(U_t^2+V_t^2+\Theta_t^2)+\tfrac{1}{2}(C_L^2U_x^2+C_T^2V_x^2+\Theta_x^2)$$

$$+\chi\cos\Theta+\alpha U_x\cos\Theta-\beta V_x\sin\Theta. \tag{11}$$

The structure of the system of nonlinear equations is of special interest. It is made of two *wave equations* for the elastic displacements (U and V) and a *sine-Gordon equation* for the rotation Θ (twice the physical dipole rotation), each equation being nonlinearly coupled. It is noteworthy mentioning that for small rotations the linearized equations (10*a*)-(10*c*) can be compared, on the one hand, to the linear equations deduced from the fully continuum approach to *ferroelectric crystals* [29] and, on the other hand, to the one-dimensional version of the elastic micropolar media [30, 31]. Moreover, the continuum approximation of the present lattice model can be also compared to the equations deduced from the nonlinear continuum model of *oriented media* [24] or *micropolar elastic crystals* [32].

Some obvious properties of the system (10) can be noted. First of all, let (U, V, Θ) be a solution for $\chi>0$. Then, (i) $(-U, -V, \pi+\Theta)$ is also a solution by changing χ into $-\chi$, so that we suppose, henceforth, that $\chi>0$, (ii) $(U, -V, -\Theta)$ and $(U, V, \Theta+2k\pi)$ are also solutions. The set of equations (10) possesses, of course, uniform static solutions

such that $U = U_0 = \text{constant}$, $V = V_0 = \text{constant}$ and $\Theta = k\pi$ $(k \in \mathbb{Z})$ which are also equilibrium points of the physical system. If the coupling coefficients are neglected the set of equation (10) reduces to the uncoupled elastic wave equations for the displacements U and V, and a sine-Gordon equation for the rotation Θ [18, 33, 34]. We notice that the following time and length scale changes $\sqrt{\chi}\, t$, $\sqrt{\chi}\, X$ and $(\alpha, \beta)/\sqrt{\chi}$ allow one to remove the coefficient χ. This means that the characteristic time and length of the nonlinear excitations is monitored by χ and, consequently, the smaller the coefficient χ the better the continuum model.

3.3. Nonlinear excitation solutions

The simplest idea is to search for solutions in the form of travelling waves, that is, a solution (U, V, Θ) to equations $(10a)$-$(10c)$ as a function of a single variable $\xi = X - X_0 - Ct$ where C is some phase velocity and X_0 is a constant. Then, we can eliminate the deformations U_ξ and V_ξ from equations $(10a)$ and $(10b)$ and substitute them into equation $(10c)$ to arrive at

$$(1 - C^2)\Theta_{\xi\xi} = -\chi(\sin\Theta + \tfrac{1}{2}\delta(C)\sin 2\Theta) \tag{12}$$

where we have defined

$$\chi\delta(C) = \frac{\beta^2}{C_T^2 - C^2} - \frac{\alpha^2}{C_L^2 - C^2}. \tag{13}$$

From the knowledge of the rotation Θ, we can compute the deformation state with

$$U_x = -\frac{\alpha}{C_L^2 - C^2}\cos\Theta \tag{14a}$$

$$V_x = \frac{\beta}{C_T^2 - C^2}\sin\Theta. \tag{14b}$$

We assume that C differs from $\mp C_L$ or $\mp C_T$. We note that the problem of nonlinear excitations of the somewhat complicated system (10) amounts to solving a nonlinear ordinary differential equation of the *double sine-Gordon* type. Thus, equation (12) possesses a first integral which is

$$\tfrac{1}{2}(1 - C^2)(\Theta_\xi)^2 = V(\Theta) - V_0 \tag{15a}$$

$$V(\Theta) = \chi(\cos\Theta + \tfrac{1}{4}\delta\cos 2\Theta) \tag{15b}$$

where V_0 is an integration constant which can be connected with the total energy of the system. The physical meaning of equation $(15a)$ is now clear, it stands for an equation governing the motion of a particle of mass $(1 - C^2)$ in the periodic potential $V(\Theta)$.

Different classes of potential $(15b)$ are plotted in figure 2 according to the value of δ (since $\chi > 0$, then $|C| < 1$ is only considered). (A) For $|\delta| < 1$, the potential (see figure $2(a)$) has equilibrium points $\Theta = \mp\pi$ which are stable while the point $\Theta = 0$ is unstable. The possible solutions to equation (15) can be qualitatively discussed on the basis of the phase trajectory diagram in the plane (Θ, Θ_ξ) given in figure 3. The corresponding trajectories are shown in figure $3(a)$: for $V_0/\chi < \delta/4 - 1$, curve (a) in figure $3(a)$ corresponds to an *aperiodic solution* with a 2π pseudo-period, this solution is drawn in figure $4(a)$ for the rotation Θ together with the deformations U_x and V_x. This result can be interpreted as a structure made of spatially periodic arrangements of domains of upward and downward dipoles separated by walls. Curve (b) in

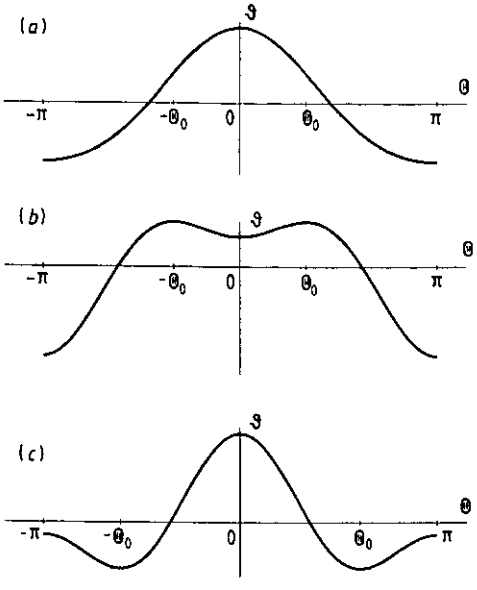

Figure 2. Configuration A: potential $V(\Theta)$ (equation (15*b*)) for (*a*) $|\delta|<1$, (*b*) $\delta<-1$ and (*c*) $\delta>1$.

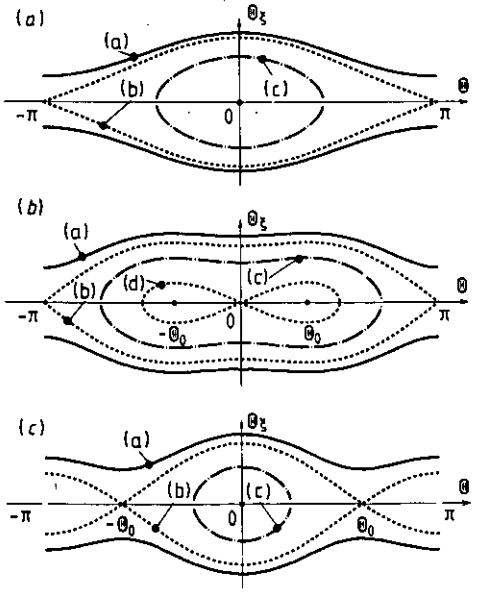

Figure 3. Configuration A: typical trajectories in the phase plane (Θ, Θ_ξ) corresponding to the potential $V(\Theta)$ (figure 2) for (*a*) $|\delta|<1$, (*b*) $\delta<-1$ and (*c*) $\delta>1$.

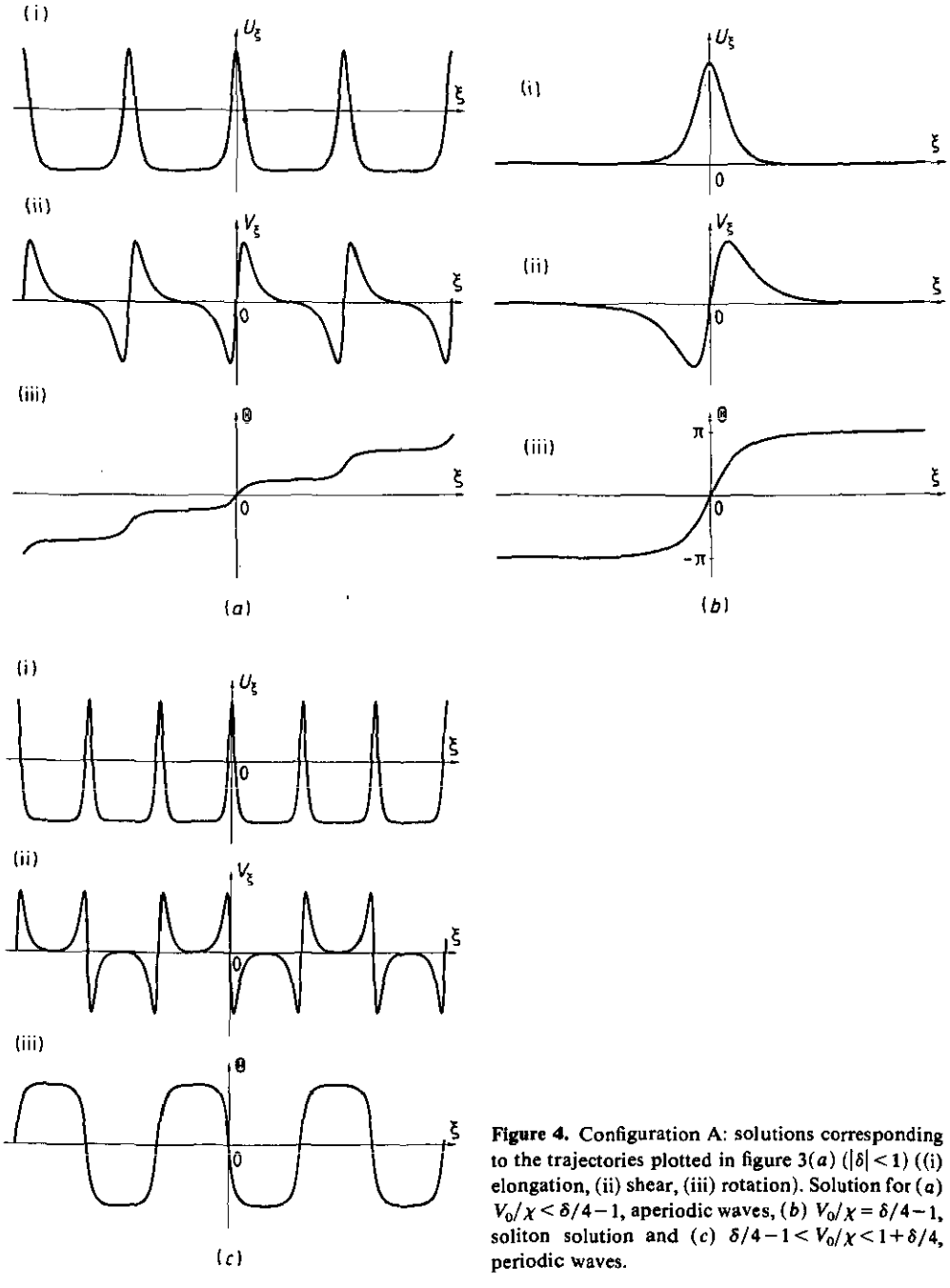

Figure 4. Configuration A: solutions corresponding to the trajectories plotted in figure 3(*a*) ($|\delta|<1$) ((i) elongation, (ii) shear, (iii) rotation). Solution for (*a*) $V_0/\chi < \delta/4-1$, aperiodic waves, (*b*) $V_0/\chi = \delta/4-1$, soliton solution and (*c*) $\delta/4-1 < V_0/\chi < 1+\delta/4$, periodic waves.

figure 3(*a*), for which $V_0/\chi = \delta/4-1$, leads to the *soliton solution* sketched in figure 4(*b*). Next, for $1+\delta/4 \geqslant V_0/\chi > \delta/4-1$, the solution is a *periodic cnoidal wave*, which can be expressed in terms of Jacobian elliptic functions. This solution, plotted in figure 4(*c*), can be seen as small domains where the dipoles perform rather large rotations from one domain to the other one. Finally, there is no solution for $V_0/\chi > 1+\delta/4$.

(B) A second situation occurs when $\delta < -1$, in this case there exists Θ_0, such that

$\cos\Theta_0 = -1/\delta$, and the potential (15*b*) (see figure 2(*b*)) has stable equilibrium points $\Theta = 0$ and $\Theta = \mp\pi$ whereas the points $\Theta = \mp\Theta_0$ are unstable. The trajectories corresponding to this case are plotted in figure 3(*b*), and, for $V_0/\chi < \delta/4 - 1$, trajectory (a) leads to an aperiodic solution as in the first situation. Figure 5(*a*) shows the solution for the rotation and deformations. For $V_0/\chi = \delta/4 - 1$, curve (b) corresponds to the soliton solution which passes through a small zone around zero where the dipoles are almost parallel to the chain axis (see figure 5(*b*)). A periodic solution is provided by trajectory (c) for $\delta/4 - 1 < V_0/\chi < 1 + \delta/4$, and this solution is drawn in figure 5(*c*). A different style of periodic solutions is illustrated in figure 5(*c'*) for V_0 such as the corresponding trajectory is close to curve (d). These periodic solutions can be considered, in fact, as an array of kink-antikink pairs travelling along the chain axis. We notice, moreover, the likeness between the half period of the periodic solutions (figure 5(*c*) or 5(*c'*)) and the solutions plotted in figure 5(*b*) or 5(*d*). A particular case, for $V_0/\chi = 1 + \delta/4$, gives curve (d) in figure 3(*b*). This yields a pulse-like soliton depicted in figure 5(*d*). Another kind of pulse soliton (still for $V_0/\chi = 1 + \delta/4$) is plotted in figure 5(*d'*), this situation will be discussed in the next subsection. At length, for $-(2+\delta^2)/4\delta > V_0/\chi > 1 + \delta/4$, we have small oscillations around the points $\mp\Theta_0$. (C) The last situation corresponds to $\delta > 1$, for which the potential (15*b*) is plotted in figure 2(*c*) and the associated trajectories are given in figure 3(*c*). The discussion is similar to that of the two preceding situations. For $V_0/\chi < -(2+\delta^2)/4\delta$, curve (a) in figure 3(*c*) is the trajectory for the aperiodic solution. The particular case $V_0/\chi = -(2+\delta^2)/4\delta$ provides the soliton solution corresponding to curve (b) in figure 3(*c*). This solution is a kink-like soliton which describes the transition from the region $\Theta = -\Theta_0$ to the region $\Theta = \Theta_0$ drawn in figure 6. Periodic solutions oscillating around either $\Theta = \mp\pi$ ($-(2+\delta^2)/4\delta < V_0/\chi < \delta/4 - 1$)) or $\Theta = 0$ ($\delta/4 - 1 < V_0/\chi < 1 + \delta/4$) correspond to curve (c) in figure 3(*c*). The aperiodic and periodic solutions corresponding to this situation have not been plotted because they are quite similar, in their form, to those presented in figures 4(*a*) and 4(*c*). Nevertheless, the particular soliton solutions can be examined with some more details for each range of δ.

3.4. Soliton solutions

Case (i). For $0 \leqslant \delta < 1$ and $V_0/\chi = \delta/4 - 1$, we have shown that equation (15*a*) possesses a kink-like solution or 2π-soliton which represents the transition from the state $\Theta = -\pi$ ($\theta = -\pi/2$, dipoles downwards) to the state $\Theta = \pi$ ($\theta = \pi/2$, dipoles upwards). By solving equations (15*a*) and (15*b*) this particular solution reads as

$$\Theta = \mp 2\tan^{-1}[\cosh\rho \sinh(\xi/l)] \tag{16a}$$

where we have set

$$l = l_0\sqrt{1 - C^2} \qquad l_0 = (\cosh\rho)/\sqrt{\chi} \qquad \delta = \tanh^2\rho. \tag{16b}$$

Moreover, the mechanical state of the lattice is given by the elongational and shear deformations computed from equations (14*a*) and (14*b*), respectively. This solution is plotted in figure 4(*b*) along with the deformations. For this case the total energy of the system can be calculated from the Hamiltonian density (11), which gives

$$E_A = \tfrac{1}{2} E_{SG}\left(\frac{(1+w)}{\cosh\rho} + (1-w)\frac{\tan^{-1}(\sinh\rho)}{\tanh\rho}\right) \tag{17a}$$

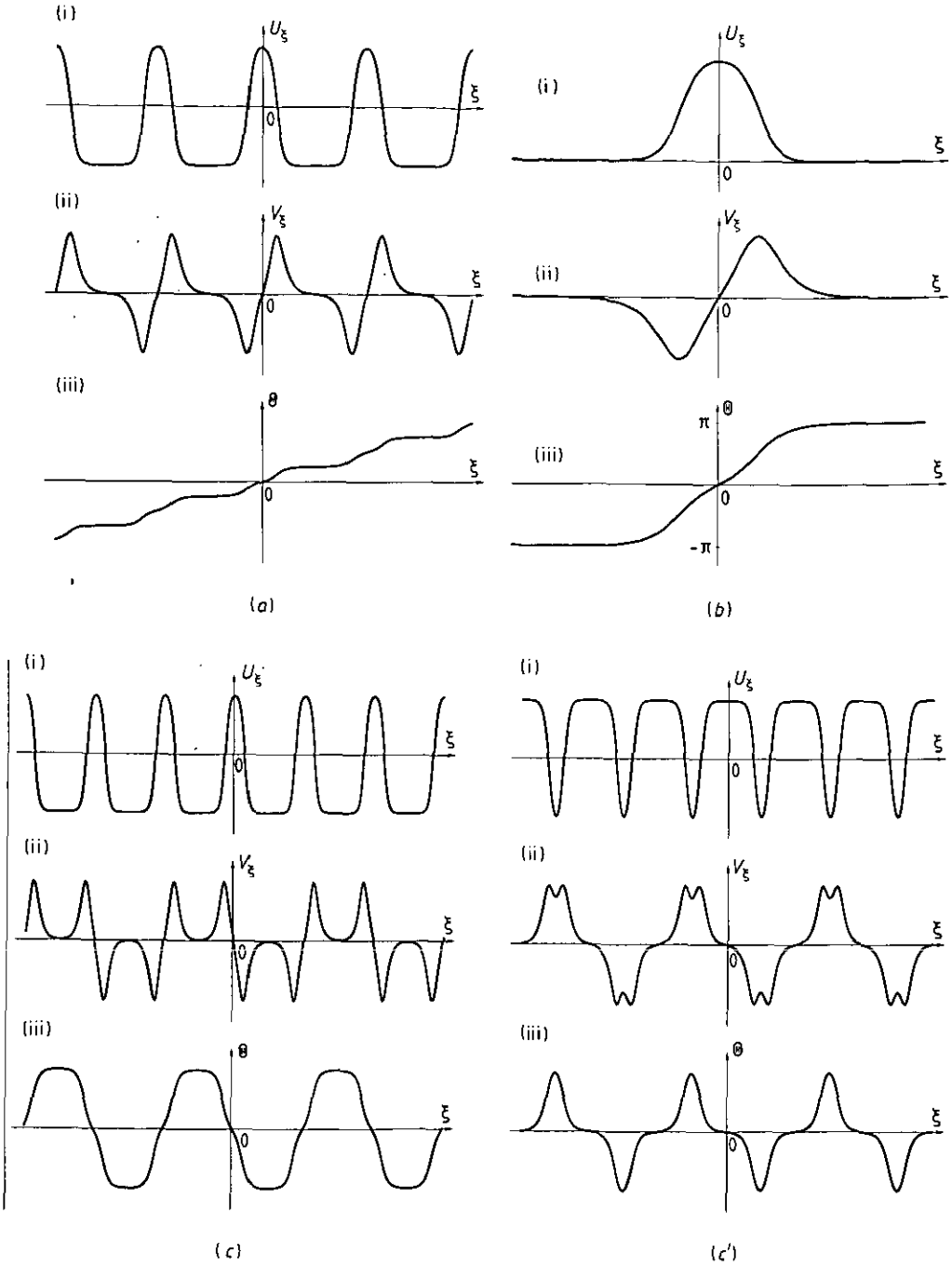

Figure 5. Configuration A: solutions in lattice deformations (i) and (ii), and rotation (iii) corresponding to the trajectories in figure 3(*b*) ($\delta < -1$) for (*a*) $V_0/\chi < \delta/4 - 1$, aperiodic solution, (*b*) $V_0/\chi = \delta/4 - 1$, kink solution, (*c*) $\delta/4 - 1 < V_0/\chi < -(2+\delta^2)/4\delta$, periodic solution (trajectory close to curve (b) in figure 3(*b*) but below), (*c'*) same conditions as in (*c*) but for a trajectory close to curve (d) in figure 3(*b*), (*d*) $V_0/\chi = 1 + \delta/4$, pulse soliton and (*d'*) same conditions as in the case (*d*) but for $\delta < -2$.

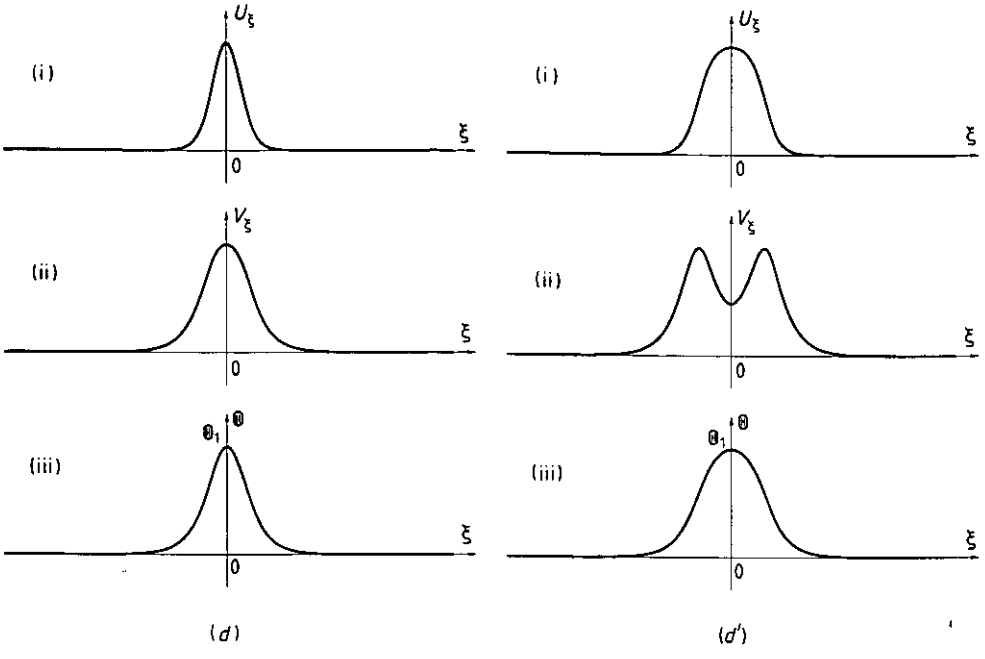

Figure 5. (continued)

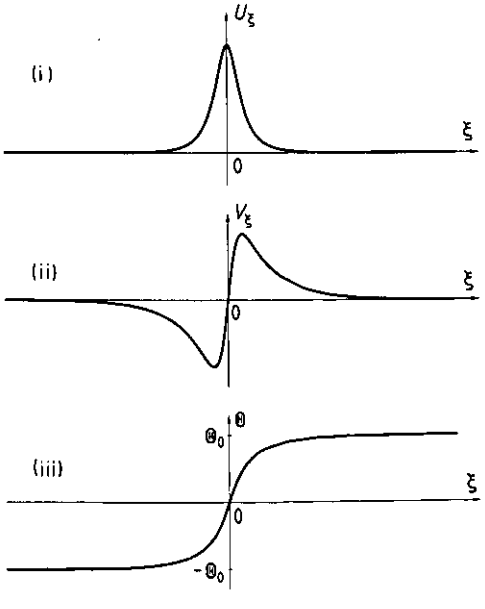

Figure 6. Configuration A: solutions in lattice deformations (i) and (ii), and rotation (iii) corresponding to curve (b) in figure 3(*c*) ($\delta > 1$) for $V_0/\chi = -(2+\delta^2)/4\delta$, 'small' kink soliton.

with

$$w = -\tfrac{1}{2}C(1-C^2)\frac{\partial}{\partial C}(\log|\delta|) \tag{17b}$$

$$E_{SG} = E_0/\sqrt{1-C^2} \qquad E_0 = 8\sqrt{\chi}. \tag{17c}$$

We note that if δ goes to zero (no coupling) the energy (17*a*) reduces to the usual energy of the sine-Gordon soliton E_{SG}. However, the energy becomes infinite when the soliton velocity approaches unity. The soliton thickness can be also obtained as

$$e = \pi l/\cosh\rho = \pi\sqrt{1-C^2}/\sqrt{\chi}. \tag{18}$$

This is a remarkable result because the soliton thickness does not depend on the coupling. This thickness tends towards zero as the velocity C goes to 1. On the other hand, when δ goes to 1, then ρ becomes infinite and the solution (16) is no longer valid. However, the limiting case can be obtained and it reads as

$$\Theta = \mp 2\tan^{-1}(\xi/l). \tag{19}$$

Case (ii). An important situation happens for $\delta < 0$, the soliton solution splits into two sine-Gordon solitons and the solution (16*a*) takes on the form

$$\Theta = \pm\tfrac{1}{2}(\Theta^-_{SG} - \Theta^+_{SG}) \tag{20a}$$

where we have set

$$\Theta^{\mp}_{SG} = 4\tan^{-1}(e^{(\Delta\mp\xi)/l}) \tag{20b}$$

$$\delta = -\sinh^2\rho \qquad \rho = \Delta/l \qquad l_0 = 1/\sqrt{\chi}\cosh\rho. \tag{20c}$$

The characteristic length l is still defined by equation (16*b*) but the length at rest differs. Taken separately, each part of the solution (20*a*) satisfies the classical sine-Gordon equation. We must point out that the soliton solution given by equations (16*a*) and (20*a*) can be compared to the 2π-soliton solution for the double sine-Gordon equation in different contexts [35-37]. Equation (20*a*) shows clearly the meaning of the parameter Δ associated with δ: the 2π-soliton solution can be considered as two π-solitons centred at $\mp\Delta$ and separated by the distance 2Δ. Figure 5(*b*) gives the soliton solution for this case. However, for $-1 < \delta < 0$, there exists only one inflexion point at $(\xi = 0, \Theta = 0)$, but for $\delta < -1$ the curve (see figure 5(*b*)) has three inflexion points at $\Theta = 0$ and $\Theta = \mp\Theta_0$. From the physical point of view, the present soliton corresponds to a *moving domain wall* which separates two domains with opposite orientations involving the lattice deformations. The total energy of the system for the solution (20) can be written as

$$E_A = \tfrac{1}{2}E_{SG}[(1-w)\cosh\rho + (1+w)\rho/\sinh\rho] \tag{21}$$

where w and E_{SG} are still given by equations (17*b*) and (17*c*). As in the previous case the energy goes to infinity as C tends towards 1 and we recover the classical energy of the sine-Gordon soliton when δ goes to zero. In the case $-1 \leqslant \delta < 0$, the soliton width is given by

$$e = \pi l\cosh\rho \tag{22a}$$

whereas for $\delta < -1$, it is defined by

$$e = 2l[\cosh^{-1}(\sinh\rho) + (\pi - \Theta_0)\tanh\rho]. \tag{22b}$$

We recall that the angle Θ_0 is such that $\cos\Theta_0 = -1/\delta$. Notice that from equations (22*a*) and (20*c*), the soliton width does not depend on the coupling, but this is not true for equation (22*b*). As it has been mentioned above, in the case $\delta < -1$ and $V_0/\chi = 1 + \delta/4$, we also have a pulse-like soliton solution (see curve (d) in figure 3(*b*)) which takes on the form

$$\Theta = \mp 2\tan^{-1}\left(\frac{\tan(\Theta_1/2)}{\cosh(\xi/l)}\right) \tag{23a}$$

with

$$2\cos\Theta_0 - \cos\Theta_1 = 1 \qquad l_0 = 1/\sqrt{\chi}\,\tan(\Theta_1/2). \tag{23b}$$

The characteristic length l is, once again, given by equation (16*b*). This solution is depicted in figure 5(*d*) together with the deformation of the lattice. From equation (23*a*), it can be seen that Θ_1 is just the maximum of the pulse-like soliton; it depends, of course, on δ or Θ_0. The energy of the system for this solution is obtained after some algebra:

$$E_A = \tfrac{1}{2}E_{SG}\{(1+w)\tan(\Theta_1/2) - (1-w)\cos(\Theta_1/2)\tanh^{-1}[\sin(\Theta_1/2)]\}. \tag{24}$$

The soliton width is computed by taking the particular shape of this soliton into account and we find

$$e = 2l\{\cosh^{-1}[\tan(\Theta_1/2)/\tan(\Theta_0/2)] + \Theta_0/\sin(\Theta_1/2)\} \tag{25}$$

where all the parameters have been defined previously. It is interesting to note that when δ goes to -1 then both Θ_0 and Θ_1 tends towards zero and the only possible solution is $\Theta = 0$. Accordingly, we can see that the soliton energy (24) goes to zero and the soliton thickness becomes infinite. Furthermore, it can be shown that the soliton solution (23*a*) is the difference of two sine-Gordon solitons as follows:

$$\Theta = \pm\tfrac{1}{2}(\Theta_{SG}^{+} - \Theta_{SG}^{-}) \tag{26a}$$

where we have

$$\Theta_{SG}^{\mp} = 4\tan^{-1}(e^{(-\xi\mp\xi_0)/l}) \tag{26b}$$

$$\sinh(\xi_0/l) = \tan(\Theta_1/2). \tag{26c}$$

Then, the decomposition carried out for the kink-like soliton holds true for the pulse-like solution as well. This decomposition is particularly striking for $\delta < -2$ for which we have a large pulse-like soliton and the soliton in shear deformation breaks into two humps as represented in figure 5(*d'*).

Case (iii). For $\delta > 1$ and $V_0/\chi = -(2+\delta^2)/4\delta$, we have shown the existence of a kink-like soliton between $-\Theta_0$ and Θ_0. This solution takes on the form

$$\Theta = \pm 2\tan^{-1}[\tan(\Theta_0/2)\tanh(\xi/l)] \tag{27a}$$

where we have put

$$\cos\Theta_0 = -1/\delta \qquad l_0 = 2/\sqrt{\chi\delta}\,\sin\Theta_0 \tag{27b}$$

and the length l is always given by equation (16*b*). This solution, which is called a 'small' kink, is plotted in figure 6. If δ goes to 1, then Θ_0 tends towards π but by means of an asymptotic expansion the solution (27) is reduced identically to equation

(19). The energy of the solution is computed from the Hamiltonian density (11) and after rather lengthy calculations we arrive at

$$E_A = \frac{E_{SG}}{4\sqrt{\delta}}[(1-w)\Theta_0 + (1+w)\tan\Theta_0] \tag{28}$$

where the energy of the sine-Gordon soliton has been introduced as in the other cases. The energy becomes infinite when the soliton velocity tends towards its upper limit. At length, the soliton thickness is given by

$$e = \Theta_0 l/\tan(\Theta_0/2). \tag{29}$$

We notice that the thickness goes to zero as the velocity tends towards 1. When δ goes to 1 we recover the limiting case met for $0 \leq \delta < 1$. As a general rule, for each case, the characteristic length l tends to zero whereas the soliton energy becomes infinite when the soliton velocity approaches its upper limit ($C \to 1$). On the other hand, we see that the problem of the one-soliton solution (both kink- and pulse-shaped solitons) to the somewhat complicated set of equations (10*a*)-(10*c*) is equivalent to the solution to the nonlinear ordinary differential equation (12) which can be formally deduced from a *double sine-Gordon equation* when a one-soliton solution is sought [36, 38]. Nevertheless, the double sine-Gordon equation is invariant under a Lorentz transformation but this is obviously not true for the system (10). This is the reason why the characteristic length l takes on a relativistic form (see equation (16*a*)) but the length at rest depends, of course, on the type of solution being considered. The same remark holds true for the energy which, for each case, is the product of the sine-Gordon soliton energy by a term involving the coupling coefficients. The energy of the sine-Gordon part (when $\delta = 0$) can be also put in a relativistic form (see equation (17*a*)) where E_0 is the energy of the soliton at rest. However, the soliton energy thus obtained for each situation cannot be deduced from the equivalent double sine-Gordon system because the energy of our physical system is computed from the Hamiltonian density (11) corresponding to the set of coupled equations (10*a*)-(10*c*) which has nothing to do with the double sine-Gordon problem.

4. Coherent structures for configuration B

4.1. Equations of motion for the discrete system

We now turn our attention to the second configuration by putting $\theta_n = \pi/2$ in the Hamiltonian (1) and energies (2)-(6). We can rewrite the Hamiltonian in terms of the angle φ_n as follows:

$$H_B = \tfrac{1}{2}\sum_n (\dot{U}_n^2 + \dot{\varphi}_n^2) + \tfrac{1}{2}\sum_n C_L^2 (U_{n+1} - U_n)^2 - \sum_n [\cos(\varphi_{n+1} - \varphi_n) - \mu\cos(\varphi_{n+1} + \varphi_n)]$$
$$+ \kappa \sum_n (U_{n+1} - U_n)\cos(\varphi_{n+1} - \varphi_n) \tag{30}$$

where we have set

$$K_L = C_L^2(-\varepsilon - \nu/2) \qquad \mu = -\nu/(2\varepsilon + \nu) \qquad \kappa = 6\varepsilon/a(2\varepsilon + \nu)$$

and where the time variable has been rescaled into $t\sqrt{-(\varepsilon + \nu/2)}$. Moreover, we assume that $\varepsilon + \nu/2 < 0$. The transverse displacements have not been considered because they

do not play any role in this situation. The equations of motion derive from equation (30) and read as

$$\ddot{U}_n - C_L^2(U_{n+1} - 2U_n + U_{n-1}) = -2\kappa \sin\left(\frac{\varphi_{n+1} - \varphi_{n-1}}{2}\right) \sin\left(\frac{\varphi_{n+1} - 2\varphi_n + \varphi_{n-1}}{2}\right) \tag{31a}$$

$$\ddot{\varphi}_n - [\sin(\varphi_{n+1} - \varphi_n) - \sin(\varphi_n - \varphi_{n-1})] = \mu[\sin(\varphi_{n+1} + \varphi_n) + \sin(\varphi_n + \varphi_{n-1})] - \kappa[(U_{n+1} - U_n)\sin(\varphi_{n+1} - \varphi_n) - (U_n - U_{n-1})\sin(\varphi_n - \varphi_{n-1})]. \tag{31b}$$

The interesting set of equations consists of a *wave equation* for the *longitudinal displacement* (equation (31*a*)) nonlinearly coupled to the dipole rotation governed by an *equation of the sine-Gordon type* (equation (31*b*)). We note that the coupling terms in equations (31*a*) and (31*b*) differ, in their nature, from those appearing in the equations for the configuration A. However, the characteristic feature of equations (31*a*) and (31*b*) will be clearer by considering the continuum approximation.

4.2. *Continuum approximation*

Using the same hypotheses as in the first configuration we can consider the continuum approximation associated with slowly extended waves with respect to the lattice spacing. Then, the set of coupled differential-difference equations becomes

$$U_{tt} - C_L^2 U_{xx} = \tfrac{1}{2}\alpha(\Phi_x)_x^2 \tag{32a}$$

$$\Phi_{tt} - \Phi_{xx} = \lambda \sin \Phi - \alpha(U_x \Phi_x)_x \tag{32b}$$

where we have set $\alpha = \kappa/2$, $\lambda = 4\mu$, $\Phi = 2\varphi$, and U has been changed into $U/2$. If the coupling between the displacement and the rotation is removed we recover the usual sine-Gordon equation [33] for the rotation and the elastic wave equation for the longitudinal displacement. However, because of the coupling, the solutions to equations (32*a*) and (32*b*) is much more complicated. It should be mentioned that the linearized equations about a steady state lead to an uncoupled system, since the coupling terms are nonlinear in space derivatives. Then, we do not recover the usual linear theory of micropolar or oriented media [21, 30].

Symmetry properties of the set (32) can be discussed; thus, let (U, Φ) be a solution to equations (32*a*) and (32*b*) for $\lambda > 0$, then, (i) $(U, \Phi + \pi)$ is a solution by changing λ into $-\lambda$, from now on we take $\lambda > 0$, (ii) $(U, -\Phi)$ and $(U, \Phi + 2k\pi)$ are also solutions to equations (32*a*) and (32*b*) and (iii) $(-U, \Phi)$ is a solution by replacing X by $-X$. Equations (32*a*) and (32*b*) have steady solutions such that $U_x = (U_x)_0$ (uniform deformation) and $\Phi = k\pi$ ($k \in \mathbb{Z}$) which are equilibrium points of the physical problem. As in the first configuration the rescaling $\sqrt{\lambda}\, t$, $\sqrt{\lambda}\, X$ and $\sqrt{\lambda}\, \alpha$ allows one to get rid of the coefficient λ from equations (32*a*) and (32*b*) and the characteristic length of the nonlinear excitations then depends on λ.

Finally, the set of equations (32*a*) and (32*b*) can be derived from the following Hamiltonian density:

$$h_B - h_0 = \tfrac{1}{2}(U_t^2 + \Phi_t^2) + \tfrac{1}{2}(C_L^2 U_x^2 + \Phi_x^2) + \lambda \cos \Phi - \tfrac{1}{2}\alpha U_x \Phi_x^2. \tag{33}$$

Note that, in the framework of the present situation, the dynamical problem of the coupled motions in rotation and elongational deformation is quite similar to that of

a compressible chain of dipoles [14] or a compressible Heisenberg chain of spins [12, 13].

4.3. Study of nonlinear excitations

We search for solutions (U, Φ) to equations (32*a*) and (32*b*) as functions of the variable $\xi = X - X_0 - Ct$ where C is the phase velocity and X_0 is some constant. Then, the first equation of the set (32) can be integrated with respect to ξ to yield

$$U_x = \frac{\alpha}{2(C_L^2 - C^2)} (\Phi_\xi)^2 + A \tag{34}$$

where A is a constant of integration and $C \neq \mp C_L$ has been assumed. On substituting equation (34) into equation (32*b*), we arrived at an equation for Φ only, which can be written as

$$4l^{-2}[l^{-2}(\Phi_\xi)^2 - a]\Phi_{\xi\xi} - \sin \Phi = 0 \tag{35a}$$

where we have set

$$l^2 = l_0^2 \left(1 - \frac{C^2}{C_L^2}\right)^{1/2} \qquad l_0^2 = \frac{2\alpha}{C_L}\sqrt{\frac{3}{\lambda}} \qquad a = \frac{1 - C^2 - \alpha A}{4\lambda} l^2. \tag{35b}$$

Equation (35*a*) can be integrated once more to yield

$$l^{-4}(\Phi_\xi)^4 - 2al^{-2}(\Phi_\xi)^2 + \cos \Phi + b = 0. \tag{36}$$

We can solve equation (36) with respect to $(\Phi_\xi)^2$ and we find

$$l^{-2}(\Phi_\xi)^2 = a - V(\Phi) \tag{37a}$$

$$V(\Phi) = \sqrt{a^2 + b - \cos \Phi}. \tag{37b}$$

We have chosen the minus sign in equation (37*a*) because the two solutions to equation (36) leads qualitatively to the same classes of nonlinear excitations. Equation (37*a*) can be associated with the motion of a particle of mass $1/l^2$ in the periodic potential (37*b*). Among the overall possible solutions to equations (37), which are mainly periodic waves, special attention is devoted to solutions such that a and b satisfy $a^2 + b - 1 \geqslant 0$, which means that the potential $V(\Phi)$ is defined everywhere. The periodic potential is drawn in figure 7 within the segment $[-\pi, \pi]$. The equilibrium points of the system are $\Phi = \mp\pi$, only if $b = 1$. The discussion of the different kinds of solutions can be qualitatively examined with the help of the trajectories in the plane (Φ, Φ_ξ), which are plotted in figure 8. If $b \leqslant -1$, there is no solution, for $b = -1$ then $\Phi = 0$ is solution. For $|b| < 1$, we have *periodic solutions* (curve (a) in figure 8). The particular case $b = 1$ corresponds to the *soliton solution* (curve (b) in figure 8) and, finally, for $b > 1$ *aperiodic solutions* exist (curve (c) in figure 8). These three types of solutions are illustrated in figure 9 (periodic wave), figure 10 (soliton solution) and figure 11 (aperiodic solution) for the rotation and deformation.

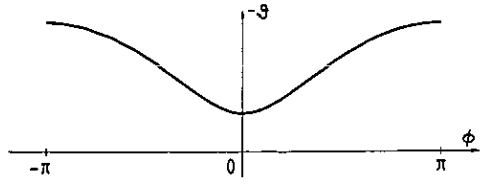

Figure 7. Configuration B: sketch of the potential $V(\Phi)$ (equation (37*b*)).

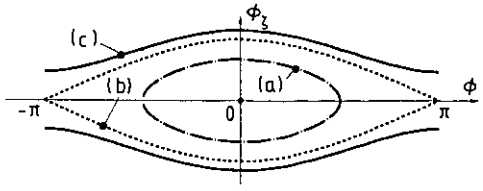

Figure 8. Configuration B: trajectories in the phase plane (Φ, Φ_ζ) corresponding to the potential drawn in figure 7 for different values of a and b.

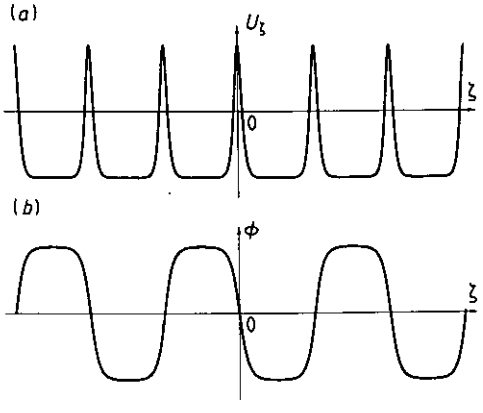

Figure 9. Configuration B: solution in (a) elongational deformation and (b) rotation for $|b|<1$, periodic solution.

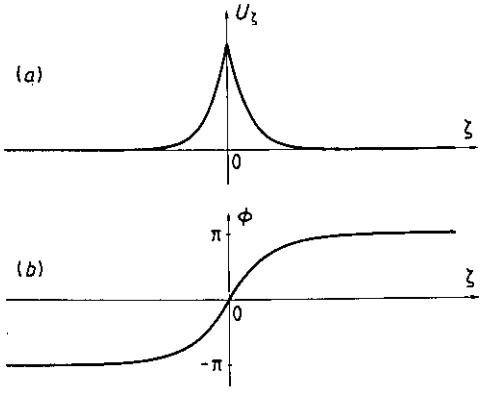

Figure 10. Configuration B: solution in (a) elongational deformation and (b) rotation for $b=1$, soliton solution.

4.4. Soliton solutions

Let us focus on a particular case for which $b=1$ and $a=\sqrt{2}$. This case allows us to reach a solution analytically and equation (37) reduces to

$$l^{-2}(\Phi_\zeta)^2=\sqrt{2}[1-|\sin(\Phi/2)|]. \tag{38}$$

Note that equation (38), within each segment $-2\pi \leqslant \Phi \leqslant 0$ and $0 \leqslant \Phi \leqslant 2\pi$, is similar

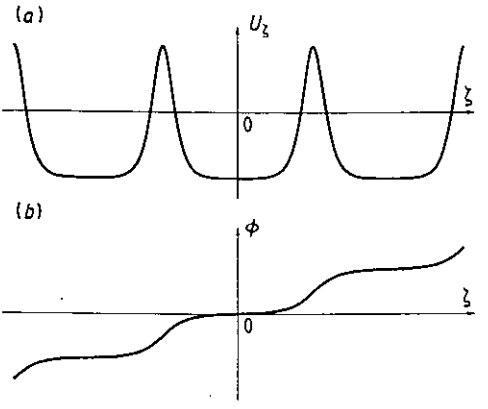

Figure 11. Configuration B: solution in (*a*) elongational deformation and (*b*) rotation for $b > 1$, aperiodic solution.

to the usual sine-Gordon equation. This equation can be solved and we find

$$\varphi = \operatorname{sign}(\xi)\left(4\tan^{-1}(e^{[(|\xi|+\Delta)/L]}) - \frac{3\pi}{2}\right) \tag{39a}$$

with

$$\Delta/L = \log(1+\sqrt{2}) \qquad L = l2^{1/4}. \tag{39b}$$

The soliton solution (39) corresponds to a rotation of the dipoles about the chain axis from the region $\varphi = -\pi/2$ ($\xi \to -\infty$) to the region $\varphi = \pi/2$ ($\xi \to \infty$). The elongation can be computed from equation (34) and it takes on a rather simple form

$$U_x = \frac{1-C^2}{2\alpha} + \frac{2\alpha}{L^2(C_L^2 - C^2)}\left[2\operatorname{sech}^2\left(\frac{|\xi|+\Delta}{L}\right) - 3\right]. \tag{40}$$

The coupled solitons in rotation and elongational deformation are drawn in figure 10. From equation (40) we can see that the elongation is mostly non-zero in both domains $\varphi = -\pi/2$ and $\varphi = \pi/2$, this means that the dipoles induce a stretching or compression along the chain axis. According to equation (40) and figure 10, we notice that the elongational deformation is a regular spiky solitary wave (or cusp soliton), since the derivative at the maximum of the amplitude is finite but it does not pass through zero. It is also interesting to note that the special choice of the constants a and b does not impose any restriction on the soliton velocity C. However, from the definition of l (see equation (35*b*)), the solution (39*a*) is valid only if $|C| < C_L$ ($C_L > 1$), which seems to be surprising in comparison with the classical sine-Gordon system for which we must have $|C| < 1$. Moreover, it is remarkable that the characteristic length l has a relativistic expression where C_L is the upper limit of the soliton velocity (see equation (35*b*)).

The soliton energy can be calculated from the Hamiltonian density (33) and after rather lengthy arithmetic we arrive at

$$E_B = 4(\sqrt{2}-1)L\lambda\left\{(\sqrt{2}+\tfrac{2}{3}) + \tfrac{1}{3}(\sqrt{2}-\tfrac{2}{3})\left(\frac{2C^2}{C_L^2 - C^2} - 1\right)\right.$$
$$\left. + \frac{2\sqrt{2}}{\lambda L^2}\left[1 + C^2 + \frac{2C^2}{C_L^2 - C^2}\left(1 - C^2 - \frac{4\lambda}{L^2}\sqrt{2}\right)\right]\right\} \tag{41}$$

which is in fact valid if $\alpha \neq 0$. The soliton width can be written as

$$e = \pi l / 2^{1/4} \tag{42}$$

which goes to zero when C tends towards C_L. When the coupling α tends towards zero the solution seems to become singular; indeed, from the definition of l and equation (36*b*) we can see that l goes to zero and the energy (41) becomes infinite. In fact, when l tends towards zero, the soliton becomes very narrow and the soliton looks like the step function: $\varphi = -\pi/2$ for $\xi < 0$ and $\varphi = \pi/2$ for $\xi > 0$; nevertheless, the continuum approximation breaks.

5. Closing remarks

The existence of nonlinear localized structures of the soliton type has been examined on the basis of an anharmonic one-dimensional lattice model made of a deformable monoatomic chain endowed with rotatory molecular groups. The nonlinear phenomena are intimately connected with the additional degrees of freedom inherent to the rotational motions of microscopic electric dipoles, which allows for particular interatomic interactions. Thus, the model accounts for the nonlinear coupling between the rotational motions and elastic deformations; hence the propagation of coupled solitons in rotation and lattice deformation. The nonlinear excitations of the soliton type studied in the present work can take place in a large variety of materials which involve a rather fine description of microstructured media with internal degrees of freedom. Thus, the above-developed model can be applied to molecular ferroelectric crystals, of which sodium nitrite provides a good candidate. Then, insofar as the structure in domains and walls is considered, the physical meaning of the soliton in rotation corresponds to a moving wall coupled to mechanical state of the lattice [39]. In addition, the physical meaning of the nonlinear periodic excitations found in section 3.1 is very close to the problem of the incommensurate-commensurate phase transitions [40]. On the other hand, the model is also suitable for polymer materials [6]. The propagation of kink solutions for such a model has been suggested in the context of the piezoelectric long chains of macromolecules of polymers such as polyvinylidene fluoride (PVF$_2$) where electric dipoles associated with the CF_2 units perform rotational motions about the chain axis [7, 8]. Another example is given by the propagating nature of the kink twist defects in crystalline polyethylene where a rotational degree of freedom is associated with the CH_2 units [6, 26]. The macromolecular structure of polytetrafluorethylene (PTFE) consisting of successive CF_2 units is also a nice physical support to the present lattice model. Moreover, extension of the model to biological macromolecules such as helical DNA can be envisaged [9, 10, 41] and for which both bending and twisting of the molecular chain must be taken into account.

As a general rule, the system both in its discrete nature and continuum version is described by a set of nonlinear equations which consists of two wave equations for the lattice displacements and a sine-Gordon equation for the rotation, these equations being nonlinearly coupled. A configuration, referred to as A, for which all the dipoles rotate about an axis perpendicular to the chain axis, is first examined and leads to the propagation of coupled solitons in rotation, elongation and shear deformation. Moreover, it has been shown that, for this configuration, the one-soliton problem of the set of nonlinearly coupled equations is equivalent to solving a double sine-Gordon equation, which in fact reduces the problem to solve a nonlinear ordinary differential

equation with respect to the phase variable. In this situation, different classes of soliton solutions are placed in evidence according to the coupling coefficients between rotations and displacements. The second configuration, referred to as B, where all the molecular groups or dipoles rotate about the chain axis is next proposed. In this case, the coupling between the rotational motion and longitudinal displacement leads to a more complicated problem and a singularity of the soliton solution appeared if the coupling tends towards zero. In addition, the consistency of every solution with the continuum approximation has been checked by means of numerical simulations on the discrete system and a good agreement has been found [28, 42].

Nevertheless, some additional work remains in various aspects. We are interested in the problem which brings into play the *combination of both configurations* A and B, and two rotational angles of the dipoles are therefore considered. In this case, we can have a complex soliton dynamic and we must examine the stability of one of the configurations with respect to small perturbations of the other configuration. Accordingly, a soliton of configuration A may be transformed, while propagating, into a soliton of configuration A and *vice versa* through the instability process. Such a situation has been pointed out in ferromagnetic crystal [43–45]. Other important solutions can be investigated by stipulating that the molecular groups or dipoles suffer small oscillations about one of the stable equilibrium points, thus creating a weak dispersion. Then, by using a semi-discrete procedure we can look for modulated-wave solutions which possess envelope solitons [46, 47]. The *influence of an external field and damping on the soliton movement* seems to be an important problem. In fact, an external field acts on the molecular groups or dipoles as a torque. This has allowed us to study the transient motion of a soliton from rest [48, 49]. At length, a more striking problem is to know how the *discreteness effects* act on the soliton dynamics. This problem is particularly well addressed by considering the influence of a time-dependent field and damping on the soliton propagation on the discrete lattice, hence the possible *transition to deterministic chaos*: this problem will be presented elsewhere.

References

[1] Michel K H and Naudts J 1978 *J. Chem. Phys.* **68** 216–28
[2] Michel K H and Courtens E 1981 *Phys. Rev.* B **23** 513–22
[3] Ishibashi Y and Takagi Y 1970 *J. Phys. Soc. Japan* **28**(suppl) 261–3
[4] Ehrhardt K D and Michel K H 1981 *Z. Phys.* B **41** 329–39
[5] Kinase K N, Makino W and Takahashi K 1985 *Ferroelectrics* **64** 173–80
[6] Skinner J L and Wolynes P G 1980 *J. Chem. Phys.* **73** 4022–5
[7] Dvey-Aharon H, Sluckin T J, Taylor P L and Hopfinger A J 1980 *Phys. Rev.* B **21** 3700–7
[8] Taylor Ph L and Banerjea A 1986 *Ferroelectrics* **66** 135–42
[9] Takeno S and Homma S 1983 *Prog. Theor. Phys.* **70** 308–11
[10] Yomosa S 1983 *Phys. Rev.* A **27** 2120–5
[11] Yomosa S 1985 *Dynamical Problems in Soliton Systems, Springer Series in Synergetics* vol 30, ed S Takeno (Berlin: Springer) pp 242–7
[12] Cieplak M and Turski L A 1980 *J. Phys. C: Solid State Phys.* **13** L777–80
[13] Fivez J 1982 *J. Phys. C: Solid State Phys.* **15** L641–3
[14] Remoissenet M 1981 *J. Phys. C: Solid State Phys.* **14** L335–8
[15] Pouget J and Maugin G A 1984 *Phys. Rev.* B **30** 5306–25
[16] de Leeuw F H, Van den Doel R and Enz U 1980 *Rep. Prog. Phys.* **43** 683–783
[17] Kleman M 1983 *Points, Lines and Walls* (New York: Wiley)
[18] Scott A C, Chu F Y F and McLaughlin D W 1973 *Proc. IEEE* **61** 1443–83
[19] Bishop A R, Krumhansl J A and Trullinger S E 1980 *Physica* **1D** 1–44

[20] Eringen A C and Suhubi E S 1964 *Int. J. Eng. Sci.* **2** 189–203
[21] Stojanovic R 1968 *CISM Lecture Notes* (Italy: Udine) pp 621–729
[22] Ericksen J L 1962 *Arch. Rat. Mech. Anal.* **9** 1–8
[23] Pouget J and Maugin G A 1989 *J. Elasticity* **22** 135–55
[24] Pouget J and Maugin G A 1989 *J. Elasticity* **22** 157–83
[25] Klein M L and McDonald I R 1982 *Proc. R. Soc. Lond.* A **382** 471–82
[26] Wahlstrand K J 1985 *J. Chem. Phys.* **82** 5247–58
[27] Bunn C W and Howells E R 1954 *Nature* **174** 549–51
[28] Pouget J 1988 *NATO-ASI Summer School: Physical Properties and Thermodynamic Behaviour of Minerals* ed E K H Salje (Dordrecht: Reidel) pp 359–402
[29] Pouget J and Maugin G A 1980 *J. Acoust. Soc. Am.* **68** 588–601
[30] Eringen A C 1968 *Fracture* vol II, ed H Liebowitz (New York: Academic) pp 621–729
[31] Askar A 1973 *J. Phys. Chem. Solid* **34** 1901–7
[32] Maugin G A and Miled A 1986 *Int. J. Eng. Sci.* **24** 1477–99
[33] Barone A, Esposito F, Magee G J and Scott A C 1971 *Revistat Del Nuovo Cimento* **1** 227–67
[34] Dodd R K, Eilbeck J C, Gibbon J D and Morris H C 1982 *Solitons and Nonlinear Wave Equations* (London: Academic)
[35] Leung K M 1983 *Phys. Rev.* B **27** 2877–88
[36] Condat C A, Guyer R A and Miller M D 1983 *Phys. Rev.* B **27** 474–94
[37] Campbell D K, Peyrard M and Sodano P 1986 *Physica* **19D** 165–205
[38] Bullough R K, Caudrey P J and Gibbs H M 1980 *Solitons, Topics in Current Physics* vol 17, ed R K Bullough and P J Caudrey (Berlin: Springer) pp 107–41
[39] Suzuki S and Takagi M 1971 *J. Phys. Soc. Japan* **30** 188–202
[40] Ishibashi Y and Shiba H 1978 *J. Phys. Soc. Japan* **45** 409–13
[41] Scott A C 1985 *Dynamical Problems in Soliton Systems* ed S Takeno (Berlin: Springer) pp 324–35
[42] Pouget J and Sayadi M K 1990 *Mechanical Modelling of New Electromagnetic Materials* ed R K I Hsieh (Amsterdam: Elsevier North-Holland) pp 179–88
[43] Kumar P 1982 *Physica* **5D** 359–69
[44] Wysin G M, Bishop A R and Kumar P 1984 *J. Phys. C: Solid State Phys.* **17** 5975–91
[45] Wysin G M, Bishop A R and Oitmaa J 1986 *J. Phys. C: Solid State Phys.* **19** 221–3
[46] Flytzanis N, Pnevmatikos St and Remoissenet M 1985 *J. Phys. C: Solid State Phys.* **18** 4603–29
[47] Remoissenet M 1986 *Phys. Rev.* B **33** 2386–92
[48] Pouget J and Maugin G A 1985 *Phys. Lett.* **109A** 389–92
[49] Pouget J 1985 *Trends in Applications of Pure Mathematics to Mechanics* (*Lecture Notes in Physics* **249**) ed E Kröner and K Kirchgässner (Berlin: Springer) pp 156–63